SEE CORRECTION FOR THIS ARTICLE
PNAS RESEARCH ARTICLE | BIOCHEMISTRY

A discrete intermediate for the biosynthesis of both the enediyne core and the anthraquinone moiety of enediyne natural products

Minakshi Bhardwaj[a], Zheng Cui[a], Erome Daniel Hankore[a], Faruk H. Moonschi[b], Hoda Saghaeiannejad Esfahani[c], Edward Kalkreuter[d], Chun Gui[d], Dong Yang[d,e], George N. Phillips Jr.[f], Jon S. Thorson[a,1], Ben Shen[d,e,g,h,1], and Steven G. Van Lanen[a,c,1]

Edited by Jon Clardy, Harvard Medical School, Boston, MA; received December 1, 2022; accepted January 30, 2023 by Editorial Board Member Stephen J. Benkovic

The enediynes are structurally characterized by a 1,5-diyne-3-ene motif within a 9- or 10-membered enediyne core. The anthraquinone-fused enediynes (AFEs) are a subclass of 10-membered enediynes that contain an anthraquinone moiety fused to the enediyne core as exemplified by dynemicins and tiancimycins. A conserved iterative type I polyketide synthase (PKSE) is known to initiate the biosynthesis of all enediyne cores, and evidence has recently been reported to suggest that the anthraquinone moiety also originates from the PKSE product. However, the identity of the PKSE product that is converted to the enediyne core or anthraquinone moiety has not been established. Here, we report the utilization of recombinant *E. coli* coexpressing various combinations of genes that encode a PKSE and a thioesterase (TE) from either 9- or 10-membered enediyne biosynthetic gene clusters to chemically complement Δ*PKSE* mutant strains of the producers of dynemicins and tiancimycins. Additionally, ^{13}C-labeling experiments were performed to track the fate of the PKSE/TE product in the Δ*PKSE* mutants. These studies reveal that 1,3,5,7,9,11,13-pentadecaheptaene is the nascent, discrete product of the PKSE/TE that is converted to the enediyne core. Furthermore, a second molecule of 1,3,5,7,9,11,13-pentadecaheptaene is demonstrated to serve as the precursor of the anthraquinone moiety. The results establish a unified biosynthetic paradigm for AFEs, solidify an unprecedented biosynthetic logic for aromatic polyketides, and have implications for the biosynthesis of not only AFEs but all enediynes.

natural products | biosynthesis | enediyne | polyketide | polyene

Enediynes are potent and broadly toxic natural products of bacterial origin (1–4). Structurally, they are characterized by a shared 1,5-diyne-3-ene system contained within either a 9-membered carbocyclic core, represented by neocarzinostatin, C-1027, and maduropeptin (Fig. 1*A*), or a 10-membered carbocycle. The latter can be further divided into two subclasses: the methyl trisulfide-containing 10-membered enediynes, represented by calicheamicin γ_1 and esperamicin A_1 (Fig. 1*B*), and the anthraquinone-fused enediynes (AFEs), represented by the founding member dynemicin A (DYN A) and the more recently discovered tiancimycin A (TMN A), uncialamycin, yangpumicin A, and sealutomicin A (Fig. 1*C*). While DYN A contains a 10-member carbocycle within a C_{14} bicyclo[7.3.1] enediyne core defined as the E and F rings, the newer AFEs lack the F ring and are characterized by C_{14} (sealutomicin A) or C_{12} (TNM A, uncialamycin, and yangpumicin A) monocyclic enediyne cores. Regardless of core size or ring architecture, the enediyne can undergo an electronic rearrangement via a Bergmann or Myers–Saito cyclization leading to a diradical species capable of crosslinking DNA or generating O_2-dependent double-stranded DNA breaks (3). This ability to damage DNA has led to the successful clinical translation of the enediynes as anticancer agents, exemplified by polymer conjugates of neocarzinostatin (SMANCS®) and antibody-enediyne conjugates of calicheamicin γ_1 (Mylotarg® and Besponsa®) (5, 6).

The complex and uniquely functionalized molecular architectures have inspired numerous biosynthetic studies aimed at deciphering the origin of the enediyne cores. Initial feeding studies with neocarzinostatin, esperamicin A_1, and DYN A were consistent with a polyketide or fatty acid origin for all enediyne cores (7, 9, 10). Cloning and characterization of representative biosynthetic gene clusters (7, 11–16) subsequently unveiled a shared gene encoding an iterative type I polyketide synthase, abbreviated PKSE, along with a gene encoding a thioesterase (TE) and three additional conserved genes of unknown function—collectively termed the minimal PKSE cassette (17, 18)—that is consistent with a polyketide origin and suggests at least some shared biosynthetic steps. Gene inactivation confirmed PKSE is essential for the biosynthesis of each class and subclass, and successful cross-complementation of

Significance

The enediyne natural products consist of a 1,5-diyne-3-ene motif within a 9- or 10-membered enediyne core. The latter includes a subclass containing an anthraquinone moiety fused to the enediyne core. Although the biosynthesis of the enediyne core and the anthraquinone moiety is known to be initiated by a polyketide synthase (PKSE), the identity of the PKSE product that is transformed to the enediyne core or the anthraquinone moiety remains speculative. A synthetic biology-chemical complementation platform was used to demonstrate that a completely deoxygenated C_{15} linear polyene is the nascent biosynthetic intermediate, one molecule of which is converted to the enediyne core while a second molecule is converted to the anthraquinone moiety, establishing an unusual biosynthetic logic for bacterial aromatic polyketides.

Author contributions: G.N.P., J.S.T., B.S., and S.G.V.L. designed research; M.B., Z.C., E.D., F.H.M., and H.S.E. performed research; E.K., C.G., and D.Y. contributed new reagents/analytic tools; M.B., F.H.M., J.S.T., B.S., and S.G.V.L. analyzed data; and E.K., D.Y., J.S.T., B.S., and S.G.V.L. wrote the paper.

The authors declare no competing interest.

This article is a PNAS Direct Submission. J.C. is a Guest Editor invited by the Editorial Board.

[1]To whom correspondence may be addressed. Email: jsthorson@uky.edu, shenb@scripps.edu, or svanlanen@uky.edu.

This article contains supporting information online at https://www.pnas.org/lookup/suppl/doi:10.1073/pnas.2220468120/-/DCSupplemental.

Published February 21, 2023.

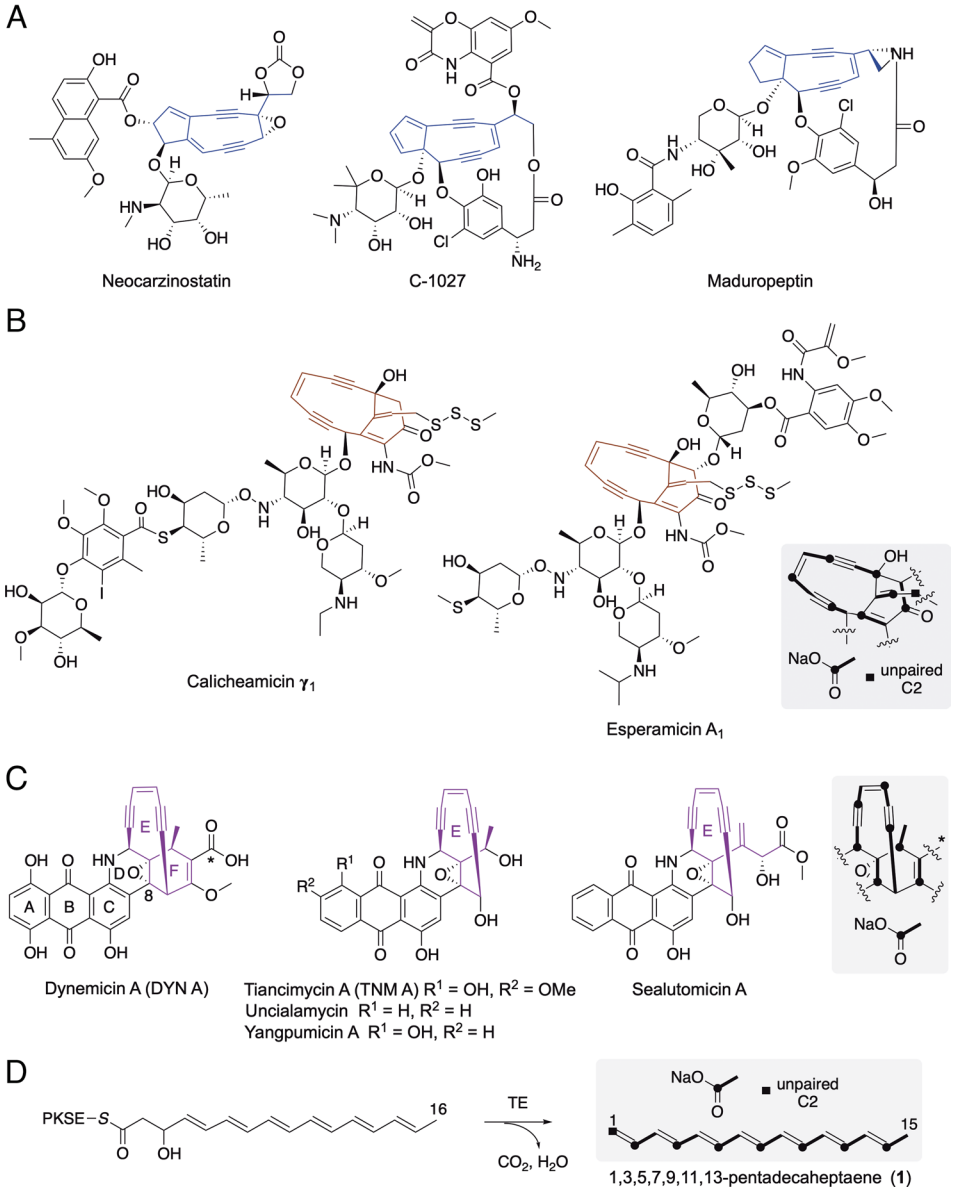

Fig. 1. Structures of selected enediynes and precursors. (*A*) Structures of representative 9-membered enediynes. The C_{14} fused bicyclic enediyne core containing the 9-membered carbocycle is highlighted in blue. (*B*) Structures of methyl trisulfide 10-membered enediynes. The C_{15} bicyclo[7.3.1]enediyne core containing the 10-membered carbocycle is highlighted in red. The observed labeling pattern of the enediyne core for esperamicin A_1 is shown. (*C*) Structures of representative anthraquinone-fused enediynes. The C_{15} bicyclo[7.3.1]enediyne core (DYN A) or C_{12}/C_{14} monocyclic enediyne cores containing the 10-membered carbocycle is highlighted in purple. The observed labeling pattern of the enediyne core for DYN A is shown. The carboxylate (*) of DYN A originates from C2 of acetate, but several lines of evidence suggest this functionality is incorporated as a tailoring step, likely migration from C8 (refs. 7 and 8). (*D*) The structure of the shared deoxygenated polyene that is derived from the PKSE/TE catalyzed reactions. The olefinic bonds are depicted in the E configurations, which has not been experimentally determined. PKSE, enediyne polyketide synthase. TE, thioesterase.

PKSE within the 9-membered enediyne class has been reported (14), consistent with an identical PKSE chemistry among the 9-membered enediynes. Insight into the biochemical function of PKSE was initially provided from biotransformation studies, wherein PKSEs involved in neocarzinostatin and C-1027 biosynthesis—when coproduced with their cognate thioesterase (TE)—were shown to produce the completely deoxygenated C_{15} polyene, 1,3,5,7,9,11,13-pentadecaheptaene (1) (19). A subsequent study revealed that PKSE/TE pairs from the 10-membered enediynes calicheamicin γ_1 and DYN A also predominantly give **1** (20). Notably, **1** production was not only dependent upon the inclusion of a TE but was independent of its source, as all PKSE/TE pairs—whether cognate or mismatched between class or subclass—produced **1** (20). Although additional mono-, di-, and tri-oxygenated polyenes have been observed (*SI Appendix*, Fig. S1), in vitro characterization of recombinant PKSE/TE pairs from C-1027, calicheamicin γ_1, and DYN A biosynthesis has been consistent with the biotransformation results, revealing **1** as the only major product that is shared between the varying enediyne classes (21–26). Furthermore, exhaustive biochemical characterization of CalE8, the PKSE involved in calicheamicin γ_1 biosynthesis, was consistent with the PKSE generating a thioesterified octaketide, 3-hydroxy-4,6,8,10,12,14-hexadecahexenoyl-*S*-PKSE (26), which could hypothetically be transformed to **1** by way of TE-mediated hydrolysis, decarboxylation, and dehydration (Fig. 1*D*) (27–29). Despite the in vivo and in vitro data that support **1** as the PKSE/TE product for all enediyne classes, direct evidence of **1** as a discrete intermediate for any enediyne has not been reported. Indeed, **1** has been commonly disregarded as an artifact without biosynthetic relevance. Instead, a PKSE-tethered C_{16} polyketide is typically

proposed as the pathway intermediate that is recognized and processed by downstream enzymes (26, 30–34).

Recently, the PKSE-catalyzed product has not only been implicated as the precursor of the enediyne core of AFEs but also the anthraquinone moiety (A–C rings, Fig. 1*C*). Genes encoding for a type II polyketide synthase (PKS), the typical biosynthetic machinery for aromatic polyketide biosynthesis in bacteria, were conspicuously absent from all known AFE biosynthetic gene clusters (15). Subsequent inactivation of eight of the nine potential PKSs encoded in the genome of the producer of DYN A revealed that production is only abolished in the PKSE (Δ*dynE8*) mutant strain, and feeding experiments revealed all O atoms of the anthraquinone moiety originate from O_2 (30). Additional experiments have revealed a C_{15} γ-thiolactone-fused iodoanthracene as the earliest known biosynthetic intermediate of the anthraquinone (*SI Appendix*, Fig. S1) (31). In support of this, a γ-thiolactone anthracene moiety in place of an anthraquinone moiety was found in the more recently discovered sungeidine A, which consists of a putative cycloaromatized 10-membered enediyne core (*SI Appendix*, Fig. S1) (34) and a gene cluster harboring a minimal PKSE cassette (8). Thus, unlike the established anthraquinone biosynthetic paradigm in bacteria, wherein a type II PKS generates a poly-β-ketoacyl-thioester intermediate that retains several of the acetate-derived oxygen atoms upon cyclization and processing (35), PKSE appears to utilize a biosynthetic logic for anthraquinone biosynthesis by furnishing a highly reduced polyketide product that is first processed to a γ-thiolactone anthracene prior to oxidation. Similar to the enediyne core, however, the identity of the PKSE product that serves as the metabolic precursor of the anthracene has not been established.

We now report on the development and implementation of a synthetic biology platform relying on interspecies chemical complementation to identify the PKSE/TE product **1** as the bona fide, earliest known discrete biosynthetic intermediate of the enediyne core as well as the anthraquinone moiety of AFEs. Using this platform technology with the DYN A and TNM A producers, it is demonstrated that the pseudosymmetrical and hydrophobic **1** is diverted into two separate pathways before reconnecting in a 1:1 ratio at a later step to make the characteristic anthraquinone-fused enediyne scaffold. Thus, the TE-catalyzed formation of **1** is an on-pathway reaction toward both C_{14} and C_{12} enediyne cores and the anthraquinone moiety, the latter supporting an unprecedented biosynthetic logic for bacterial aromatic polyketides that originate from a linear, completely deoxygenated polyene. As discussed, the results now enable us to expand upon and solidify a unified biosynthetic pathway for the AFE family of enediynes that starts with **1** and proceeds through an enediyne core with an intact F ring. Furthermore, **1** produced from 9-membered enediyne PKSE/TE pairs is shown to chemically restore AFE production, consistent with our prior hypothesis that PKSE chemistry does not direct biosynthetic divergence among the enediyne classes. Thus, consistent with the cumulative evidence to date, we propose herein that **1** is the discrete intermediate of all enediyne cores. The described platform now enables downstream studies aimed at deciphering the remaining catalytic steps directing the transformation of **1** to the enediyne core and anthraquinone moieties of AFEs and will also serve as inspiration for interrogating a unified enediyne core biosynthetic paradigm.

Results

Establishment of an Interspecies Chemical Complementation System. The evidence to date that the TE plays an integral role in processing the PKSE product is consistent with a discrete polyene intermediate being formed during enediyne core biosynthesis. We therefore reasoned that minimally one of the previously identified polyenes would be able to chemically complement a PKSE mutant strain. The TNM A producer *Streptomyces sp.* CB03234 and its PKSE mutant (Δ*tmnE*) mutant strain SB20001 were chosen as the model hosts in part because i) the structure of TNM A contains two polyketide-derived components, the enediyne core and anthraquinone moiety, that can simultaneously be interrogated and ii) the relatively high and reproducible titer of TNM A and related metabolites from the wild-type strain and various mutants (16, 36–39). HPLC analysis of fermentations confirmed the wild-type production of TNM A, the identity of which was supported by MS and NMR spectroscopic analyses of the purified enediyne, and the production of TNM A was abolished in the mutant strain SB20001 as previously reported (*SI Appendix*, Fig. S2) (16).

With the host in hand, we next aimed to prepare hypothetical post-PKSE intermediates for chemical complementation. Several technical challenges toward the synthesis of the known PKSE-associated polyenes were quickly realized. Notably, as has been well documented in the literature (25, 40–42), unsubstituted linear polyenes exceeding five conjugated double bonds are sparingly soluble and highly unstable, degrading or polymerizing rapidly even under anoxic and dark environs. Therefore, a more expedient approach for obtaining the enediyne core precursor was desired. The ability to obtain a fully operational PKSE in *E. coli* (19, 21–26), which could serve as the foundation for the identification of the various polyenes led us to entertain the possibility of using genetically defined, recombinant *E. coli* strains expressing PKSE ± TE genes as synthetic factories for precursor production. Importantly, coproduction of PKSE with any enediyne TE produced exclusively **1** (20) and thus would be excellent starting points for probing the biosynthetic relevance of **1**, if any (Fig. 2*A*).

The PKSE (DynE8) and TE (DynE7) involved in DYN A biosynthesis were initially selected because DYN A and TNM A consist of the same structural components with minor variations that are likely a consequence of late-stage functionalization. Identical to our reported data (20), coexpression of *dynE8* and *dynE7* yielded an *E. coli* strain that produced one major polyene at a retention time of 27.8 min that was not present in the control strains, including a strain expressing only *dynE8* (*SI Appendix*, Fig. S3). The UV/Vis spectrum was the same as that reported for **1** with a diagnostic fine spectrum with λ maxima of decreasing intensities at 396 nm, 374 nm, and 354 nm (*SI Appendix*, Fig. S3) (19). However, neither the expected ion for **1** nor any other characterized polyene was detected by LCMS (either ESI or APCI; *SI Appendix*, Fig. S3) or GCMS (*SI Appendix*, Fig. S4). Nevertheless, the yellow, insoluble debris from *E. coli* coexpressing *dynE8* and *dynE7* was sonicated, repeatedly washed, and fed to SB20001. LC–MS of the fermentation extract yielded an ion peak at a retention time identical to authentic TNM A (*SI Appendix*, Fig. S5). The peak gave an $[M + H]^+$ ion of m/z = 486.2160, which is consistent with that expected for TNM A (calculated m/z = 486.1189) and, critically, was absent in control experiments when feeding an extract from an *E. coli* strain expressing only *dynE8* (*SI Appendix*, Fig. S5). Although yields were very low, the data established proof of concept that a recombinant *E. coli* strain could be used to produce an enediyne biosynthetic intermediate that can successfully chemically complement a PKSE mutant strain. Additionally, the results demonstrated that a PKSE from a 10-membered enediyne can functionally complement a PKSE of the same subclass.

Chemical Complementation between 9- and 10-Membered Enediynes. We next interrogated whether *E. coli* strains coexpressing *sgcE* and *sgcE10*, which encode the respective PKSE and TE involved

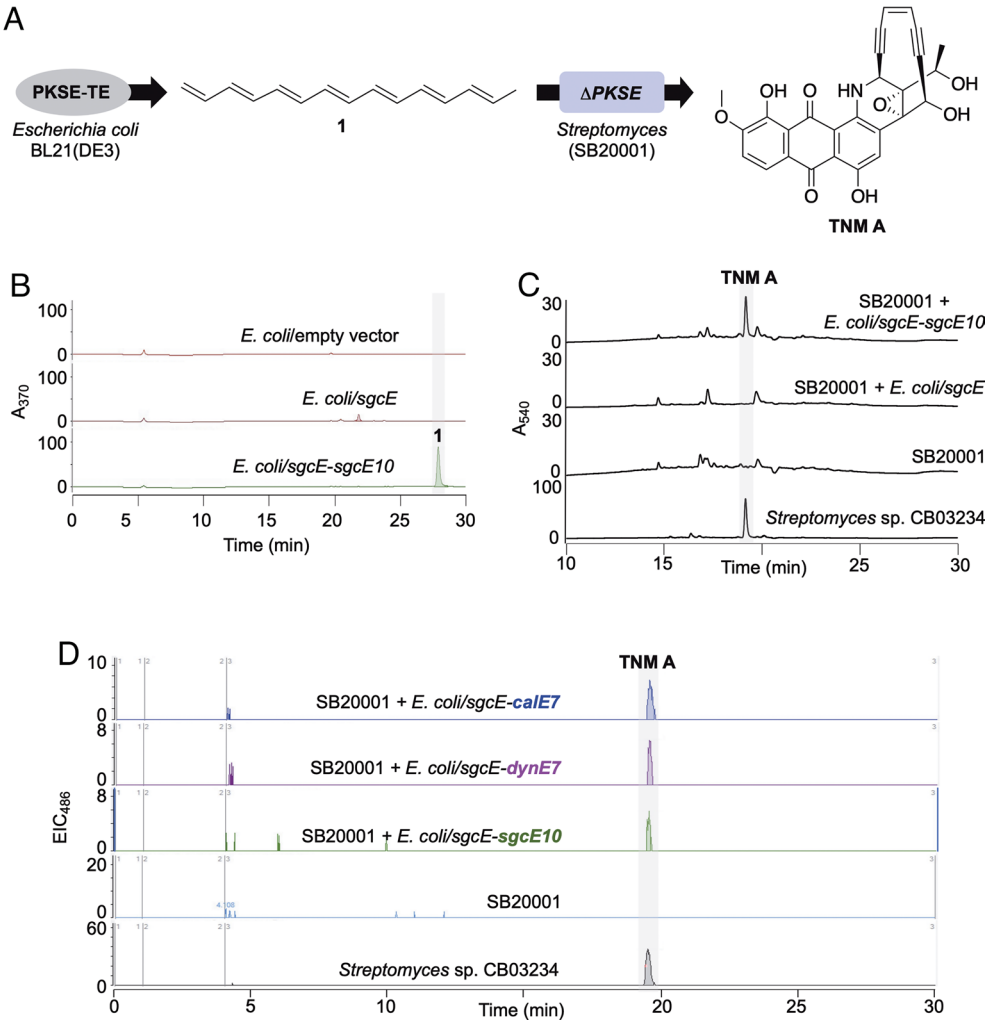

Fig. 2. Chemical complementation for enediyne biosynthesis. (*A*) Schematic representation of the production of enediyne precursor 1,3,5,7,9,11,13-pentadecaheptaene (**1**) in *E. coli* coproducing PKSE and TE, and conversion of **1** into tiancimycin A (TNM A) by the Δ*PKSE* mutant strain SB20001. The olefinic bonds of **1** are depicted in the *E* configuration, which has not been confirmed experimentally. (*B*) HPLC traces of extracts of *E. coli* expressing *sgcE* (encoding PKSE) with or without *sgcE10* (encoding TE). A_{370}, absorbance units ($\times 10^{-3}$) at 370 nm. (*C*) HPLC traces of fermentation extracts from *Streptomyces* sp. CB03234 (wild-type TNM A producing strain), SB20001 (Δ*PKSE* = Δ*tnmE*), and SB20001 supplemented with the extracts of *E. coli* expressing the indicated gene(s). A_{540}, absorbance units ($\times 10^{-3}$) at 540 nm. (*D*) HPLC traces of fermentation extracts from *Streptomyces* sp. CB03234, SB20001, and SB20001 supplemented with the extracts of *E. coli* expressing *sgcE* with different TE-encoding genes. EIC_{486}, extracted ion chromatogram ($\times 10^2$) at *m/z* = 486.1. PKSE, enediyne polyketide synthase; TE, thioesterase.

in the biosynthesis of the 9-membered enediyne C-1027, could chemically complement SB20001 and restore TNM A production (Fig. 2). From our experience working with PKSE and TE pairs, yields of **1** from *E. coli* coexpressing *sgcE* and *sgcE10* were significantly higher than others (20). Thus, if successful, this would not only demonstrate that 9- and 10-membered enediyne PKSE/TE pairs are interchangeable but would provide a robust complementation system for downstream studies. As expected, coexpression of *sgcE* and *sgcE10* yielded a strain that produced exclusively **1** (Fig. 2*B* and *SI Appendix*, Fig. S6), which was readily identifiable by comparisons with published chromatographic and spectroscopic data (19, 20, 22, 25). Although APCI yielded a minor $[M + H]^+$ ion at *m/z* = 199.1484 tenuously assigned to **1** (*SI Appendix*, Fig. S6), GCMS provided an incontrovertible, major molecular ion (M^+) peak at *m/z* = 198.1 (*SI Appendix*, Fig. S7) and a tractable fragmentation pattern that was consistent with a conjugated double-bond system and the overall structure of **1** (*SI Appendix*, Fig. S8). No other PKSE-associated polyenes were detected. When prepped insoluble debris from the *sgcE*/*sgcE10* coexpression strain was fed to SB20001, HPLC analysis revealed the restoration of TNM A production, which was confirmed by HRMS (Fig. 2*C*). Using the identical preparative conditions, coexpression of the *sgcE*/*sgcE10* pair compared with the *dynE8*/*dynE7* pair yielded minimally a 10-fold increase in production of TNM A. A control strain expressing only *sgcE* was unable to restore TNM A production (Fig. 2*C*), confirming that the coexpression of the TE gene with the PKSE gene is essential. The requirement of the TE suggests that, unlike the proofreading role assigned to most type II TEs involved in thiotemplated assembly lines (43–45), enediyne TEs have a direct biosynthetic role by producing a discrete, on-pathway intermediate.

The improved yield of **1** using the *sgcE*/*sgcE10* coexpression strain enabled additional experiments to interrogate enediyne core biosynthesis. Thus, the same approach was used to chemically cross complement the Δ*dynE8* mutant strain that was previously generated from the DYN A producer (15). As expected, feeding of the insoluble debris of *E. coli* coexpressing *sgcE* and *sgcE10* to the Δ*dynE8* mutant yielded a peak with the same retention time, UV/Vis spectrum, and MS spectrum as authentic DYN A (*SI Appendix*, Figs. S9 and S10). In combination with chemical complementation to restore the production of TNM A, the results firmly establish that the 9-membered enediyne PKSE is functionally equivalent to the PKSE from the AFE subclass. To further

dissect the requirements for cross-complementation, *sgcE* was also coexpressed with *dynE7* or *calE7*, the latter encoding the TE involved in calicheamicin γ_1 biosynthesis, and the processed cell debris was fed to SB20001. Regardless of the TE source, the production of TNM A was restored (Fig. 2*D*), which is consistent with the prior results showing that all PKSE/TE pairs produce **1**. Thus, structural divergence to the AFE enediyne core must occur after the formation of a shared PKSE/TE product. This conclusion is consistent with the prediction put forth based on our structural analysis of TEs (29).

To enhance the utility of the approach, the interspecies chemical complementation platform was further optimized. The timing of feeding was found to be important for optimal biotransformations, and early time points during the fermentation gave optimal yields (*SI Appendix*, Fig. S11). Next, several work-up conditions for *E. coli* coexpressing *sgcE*/*sgcE10* were screened. Whether using an ethyl acetate extraction of the insoluble material or a protease-treated insoluble debris, chemical complementation was successful (*SI Appendix*, Fig. S11), providing additional evidence that a protein-free small molecule restores TNM A production. However, consistent with the labile nature of **1**, the additional processing such as ethyl acetate extraction diminished the yield. In total, the data support **1** as the PKSE/TE product that is a discrete biosynthetic intermediate for the AFE enediyne core.

The PKSE/TE Product Is the Precursor of the Enediyne Core and Anthraquinone Moiety. Isotopic enrichment studies using [1-^{13}C]acetate or [2-^{13}C]acetate were performed to firmly establish that the enediyne core and anthraquinone moiety of TNM A each originate from the same PKSE/TE product **1**. *E. coli* cells coexpressing *sgcE* and *sgcE10* were fed [1-^{13}C]acetate, and the incorporation into **1** was analyzed by GCMS (Fig. 3*A*). When compared with natural abundance **1**, a series of ions ranging up to M + 7 was observed (Fig. 3*A* and *SI Appendix*, Fig. S12), consistent with the incorporation of seven acetate units to form [2,4,6,8,10,12,14-^{13}C]**1**. The data fitted well to a binomial distribution considering each C_2 extension—i.e., the incorporation of one acetate unit—as an independent event with success defined as incorporation of one ^{13}C. Since the eighth acetate unit undergoes decarboxylation to generate **1** (Fig. 3*A*), successful incorporation of [1-^{13}C]acetate for the terminal event is not detected and hence is not considered in the distribution. The probability of success, which was equated to the percent enrichment, ranged from 55 to 82% depending on the replicate and experimental conditions (representative data shown in *SI Appendix*, Fig. S12). Feeding with [2-^{13}C]acetate revealed a series of ions ranging up to M + 8 (Fig. 3*B*), consistent with the incorporation of eight acetate units to form [1,3,5,7,9,11,13,15-^{13}C]**1**. The data similarly fitted well to a binomial distribution of eight independent trials (Fig. 3*B*), with a range of 64 to 82% enrichment (*SI Appendix*, Fig. S12).

Labeled [2,4,6,8,10,12,14-^{13}C]**1** (82 ± 3% enriched) from [1-^{13}C]acetate was then fed to SB20001. The production of TNM A was restored with an $[M + H]^+$ ion distribution ranging from +3 to +13, consistent with two molecules of **1** combining to form one molecule of TNM A (Fig. 3*C*). The HRMS data were fitted to a binomial distribution with n = 13 (13 ^{13}C originating from [1-^{13}C]acetate via [2,4,6,8,10,12,14-^{13}C]**1**) (Fig. 3*C*). The probability of success was calculated to be 79 ± 2%, which is identical (within error) to the enrichment of [2,4,6,8,10,12,14-^{13}C]**1** calculated by GCMS, suggesting that **1** is the only source of both the enediyne core and the anthraquinone moiety of TNM A. The same general process was used to analyze the feeding results using [1,3,5,7,9,11,13,15-^{13}C]**1** (81 ± 2% enriched) derived from [2-^{13}C]acetate (Fig. 3*D*). HRMS of labeled TNM A similarly gave an $[M + H]^+$ ion distribution ranging from +3 to +13. Fitting the data gave a probability of success of 79 ± 2%, likewise suggesting that two molecules of [1,3,5,7,9,11,13,15-^{13}C]**1** are diverted independently into two pathways, one to furnish the enediyne core and the other to generate anthraquinone moiety.

The production of TNM A from [1-^{13}C]acetate via [2,4,6,8,10,12,14-^{13}C]**1** (Fig. 3*C*) was scaled up, and ^{13}C NMR of purified TNM A revealed an enrichment of seven carbons in the anthraquinone moiety and six carbons in the enediyne core with a clear coupling (J = 58.75 Hz) between C15 of the anthraquinone and C16 of the enediyne core (Fig. 3*E* and *SI Appendix*, Fig. S13). Peak assignments were consistent with the identity of [$^{13}C_{13}$]TNM A as [3,5,7,9,11,13,15,16,18,20,22,24,26-^{13}C]TNM A, the enrichment sites of which were identical to prior acetate feeding experiments within the wild-type producing strains of AFEs (7, 34, 37). The production of labeled TNM A from [2-^{13}C]acetate via [1,3,5,7,9,11,13,15-^{13}C]**1** (Fig. 3*D*) was likewise scaled up, and ^{13}C NMR revealed enrichment of 13 distinct carbons, seven carbons assigned to the anthraquinone and six carbons to the enediyne core. Peak assignments were consistent with the identity of the [$^{13}C_{13}$]TNM A isotopologue as [2,4,6,8,10,12,14,17,19,21,23,25,27-^{13}C]TNM A (Fig. 3*E* and *SI Appendix*, Fig. S14).

Evidence That Two Molecules of 1 Generate One Molecule of TNM A. Unlike the other potential enediyne precursors (Fig. 1*D* and *SI Appendix*, Fig. S1), **1** does not have directionality imposed by a heteroatom. Considering this and the low energy barrier inherent with these types of conjugated π-systems (40–42), we hypothesized that **1** could tautomerize (generating **1′**) during processing and feeding (Fig. 4*A*). This tautomerization would alter the polyketide orientation and, if observed, would lend additional support for **1** as the intermediate. Despite a change in orientation with respect to the starter acetate unit (C_2 unit C14-C15 of **1** becomes C2-C1 of **1′**), the symmetry of **1** derived from [1-^{13}C]acetate or [2-^{13}C]acetate results in the same labeling pattern and ion distribution when comparing the hypothetical tautomers (Fig. 4*A*). Similarly, processing of either **1** tautomer derived from [1-^{13}C]acetate or [2-^{13}C]acetate into the anthraquininone moiety or enediyne core yields the identical sites of enrichment in TNM A that cannot be distinguished analytically. Contrastingly, a distinct enrichment pattern should be observed for TNM A starting from [1,2-^{13}C]acetate if tautomerization of **1** was occurring (Fig. 4*A*). Notably, **1** incorporated without tautomerization yields a total of 13 C_2 units in TNM A derived from intact [1,2-^{13}C]acetate, and hence only $[M + 2y + H]+$ ions, where $0 \leq y \leq 13$, should be theoretically observed (Fig. 4*A*). If one or both moieties instead originate from the tautomer **1′**, C-C bond breaks occur within intact acetate-derived units to yield only 11 or 12 C_2 units in TNM A derived from intact [1,2-^{13}C]acetate, resulting in distinctive distribution patterns consisting of $[M + y + H]+$ ions, where $0 \leq y \leq 26$ (Fig. 4*A*).

Feeding [1,2-^{13}C]acetate to *E. coli* coexpressing *sgcE* and *sgcE10* yielded **1** with a series of ions ranging up to M + 15, consistent with the incorporation of eight acetate units with decarboxylation of the terminal acetate to form [U-^{13}C]**1** (Fig. 4*B*). For this labeling experiment, the final decarboxylation dictates the observed ions such that ^{13}C incorporation (a success) in the terminal unit results in odd ion peaks while natural abundance incorporation (a failure) yields even ion peaks. Given the high chance of success of enrichment that was determined from feeding [1-^{13}C]acetate and [2-^{13}C]acetate, a predominance of odd-charged ions was expected, which is exactly what is observed (Fig. 4*B*). Fitting the data to a binomial distribution reflecting the decarboxylation

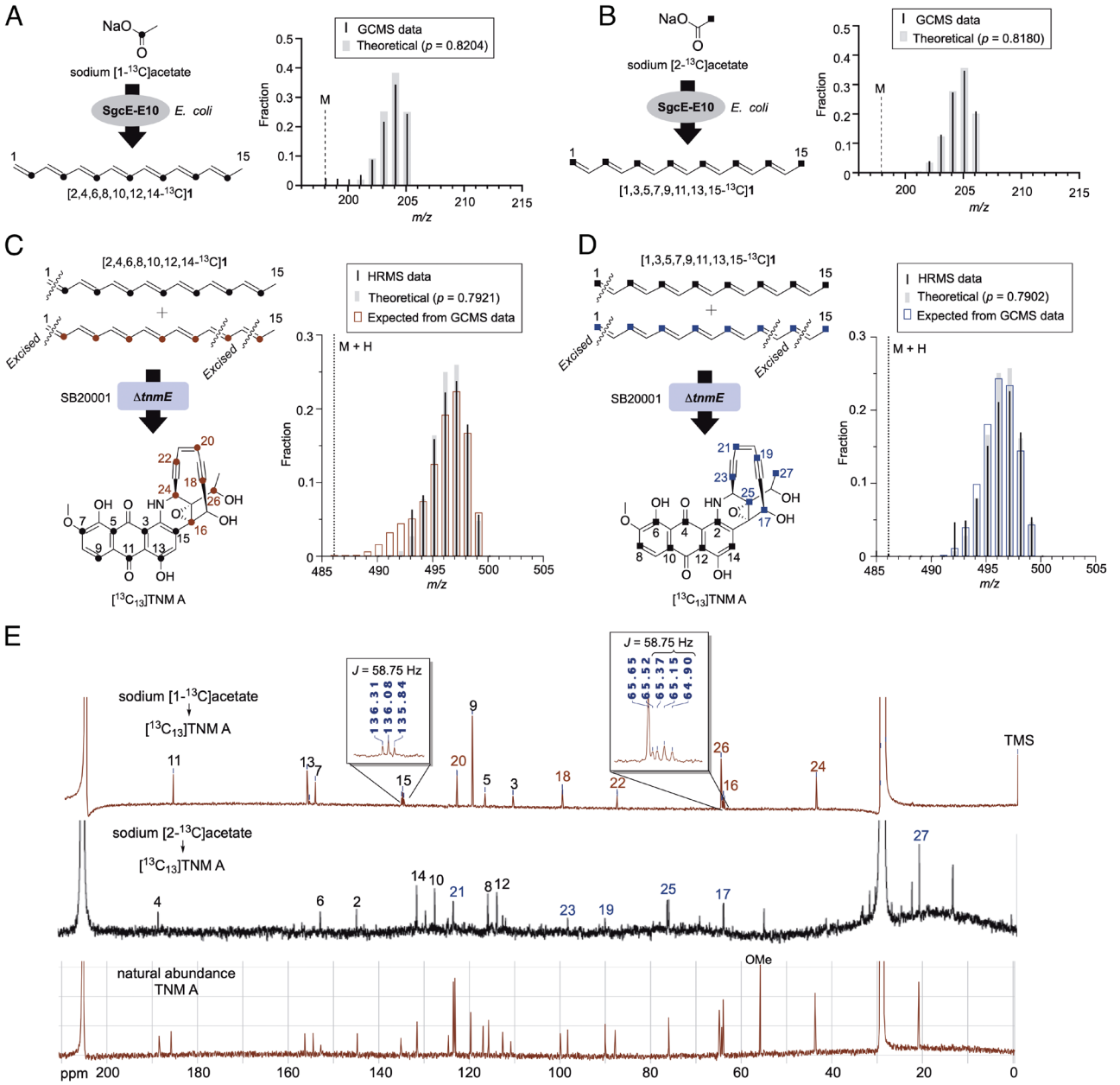

Fig. 3. Enrichment from singly labeled acetate. (*A*) Expected labeling pattern of **1** from [1-^{13}C]acetate and mass spectrum following feeding. *P*, the probability of success of incorporating one ^{13}C in a given trial. (*B*) Expected labeling pattern of **1** from [2-^{13}C]acetate and mass spectrum following feeding. *P*, the probability of success of incorporating one ^{13}C in a given trial. (*C*) Expected labeling pattern of TNM A derived from [2,4,6,8,10,12,14-^{13}C]**1** and mass spectrum following feeding. *P*, the probability of success of incorporating one ^{13}C per trial. The theoretical distribution was determined from the indicated probability that was calculated by fitting the data to a binomial distribution of n = 13, and the expected distribution pattern is derived from 82%-enriched [2,4,6,8,10,12,14-^{13}C]**1**. (*D*) Expected labeling pattern of TNM A derived from [1,3,5,7,9,11,13,15-^{13}C]**1** and mass spectrum following feeding. *P*, the probability of success of incorporating one ^{13}C per trial. The theoretical distribution was determined from the indicated probability that was calculated by fitting the data to a binomial distribution of n = 13, and the expected distribution pattern is derived from 81.8%-enriched [1,3,5,7,9,11,13,15-^{13}C]**1**. (*E*) ^{13}C-NMR spectra of natural abundance TNM A (*Bottom*); TNM A from feeding [1-^{13}C]acetate via [2,4,6,8,10,12,14-^{13}C]**1** (*Top*); and TNM A from feeding [2-^{13}C]acetate via [1,3,5,7,9,11,13,15-^{13}C]**1** (*Middle*).

event revealed 75% enrichment, comparable to the other feeding results. When the extract containing [U-^{13}C]**1** (75% enriched) was fed to SB20001, the production of TNM A was restored, giving an ion distribution ranging from +9 to +26 (Fig. 4*C*), further confirming the results from singly labeled acetate feeding experiments that the enediyne core and anthraquinone moiety originate from two molecules of the same polyketide precursor. Examination of the ion distribution revealed both even and odd ions, which is consistent with some tautomerization of **1** prior to incorporation into the enediyne core, anthraquinone moiety, or both (Fig. 4*A*). The ion distribution fitted best to a model considering an equal abundance of **1** tautomers with an unbiased incorporation into either structural component to yield four isotopologues each representing 25% of the total TNM A (Fig. 4*C*).

Given the prior reports deciphering the enrichment pattern of AFEs (7, 34, 37), we hypothesize that tautomerization is an artifact of the work-up procedures that is probably not realized within native producers. In support of this, processing of the GCMS data of [U-^{13}C]**1** to reflect tautomerization gave an expected distribution that overlapped with the observed distribution in TNM A (Fig. 4*C*), suggesting that the tautomerization can occur prior to feeding of SB20001. Although additional studies are needed to interrogate **1** tautomerization, the results from doubly labeled acetate clearly support **1**—in contrast to the other PKSE-associated

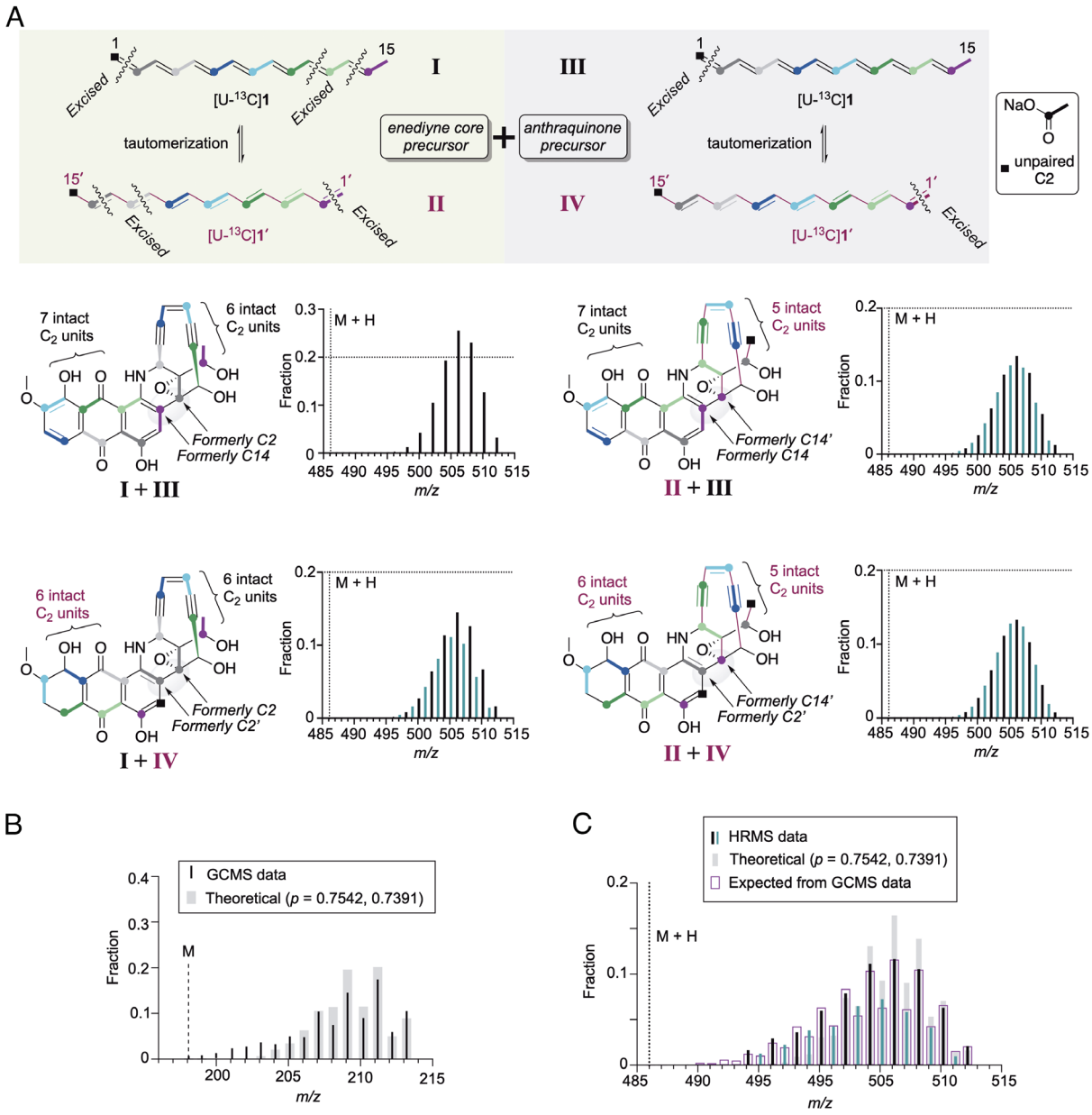

Fig. 4. Enrichment of TMN A from [1,2-^{13}C]acetate. (*A*) Labeling of [U-^{13}C]**1** and the tautomer [U-^{13}C]**1′** originating from [1,2-^{13}C]acetate. (*A*) Processing of [U-^{13}C]**1** with or without tautomerization to give the enediyne core and anthraquinone moiety. The thick bond represents two ^{13}C originating from intact [1,2-^{13}C]acetate, the circles indicate ^{13}C originating from C1 of acetate, and the black square indicates the remaining ^{13}C from C2 of the initiating acetate following decarboxylation. Carbons eliminated during processing are labeled as excised. The roman numerals are used to designate the precursor with the depicted processing route that is used during TMN A biosynthesis. The structures of the four potential isotopologues are shown alongside the theoretical mass distribution assuming 100% of incorporation of the indicated precursor. (*B*) Mass spectrum of [U-^{13}C]**1** following feeding. *P*, the probability of success of incorporating one $^{13}C_2$ per trial. The theoretical distribution was determined from the indicated probability that was calculated by fitting the data to binomial distributions of n = 7 and n = 8, respectively. (*C*) Mass spectrum of TMN A following feeding with [U-^{13}C]**1**. The expected distribution pattern is derived from the distribution for [U-^{13}C]**1** shown in panel *B*. The theoretical distribution is for a 1:1:1:1 mix of the four isotopologues depicted in panel *A*.

polyenes—as the discrete PKSE/TE product that is independently processed to the AFE enediyne core and anthraquinone moiety.

Discussion

We have employed a synthetic biology-chemical complementation platform to demonstrate that **1** is a biosynthetic precursor of DYN A, a C_{14} bicyclo[7.3.1]enediyne core-containing AFE, and TNM A, a representative of the C_{12} monocyclic enediyne core-containing AFEs. These results, along with the several biogenic analogues of TNM A that have been isolated from gene inactivation studies, allow us to propose a unified biosynthesis of the enediyne cores of AFEs starting from the PKSE/TE product **1** (Fig. 5). We recently generated a Δ*tnmK1* mutant strain that led to the isolation of the earliest known enediyne-containing precursor of TNM A, TNM H, that contains a bicyclo[7.3.1]enediyne core reminiscent of DYN A (37). In addition to the intact F ring, TNM H also contains a cryptic aldehyde functionality that is not found in DYN A, and feeding experiments revealed the aldehyde functionality originates from an unpaired C2 of acetate followed by fourteen carbons originating from seven head-to-tail acetate units (37). The carbon chain length and labeling pattern of TNM H is consistent with **1** as an upstream precursor and establishes the most likely folding pattern to furnish the enediyne core. Thus, **1** is proposed to undergo cyclization between C2-C11 and C3-C14 to form a bridged bicyclic core (Fig. 5, path a) with C4 of **1** bonded to a precursor of the anthraquinone moiety via a ring junction N atom. Although the timing of enediyne core

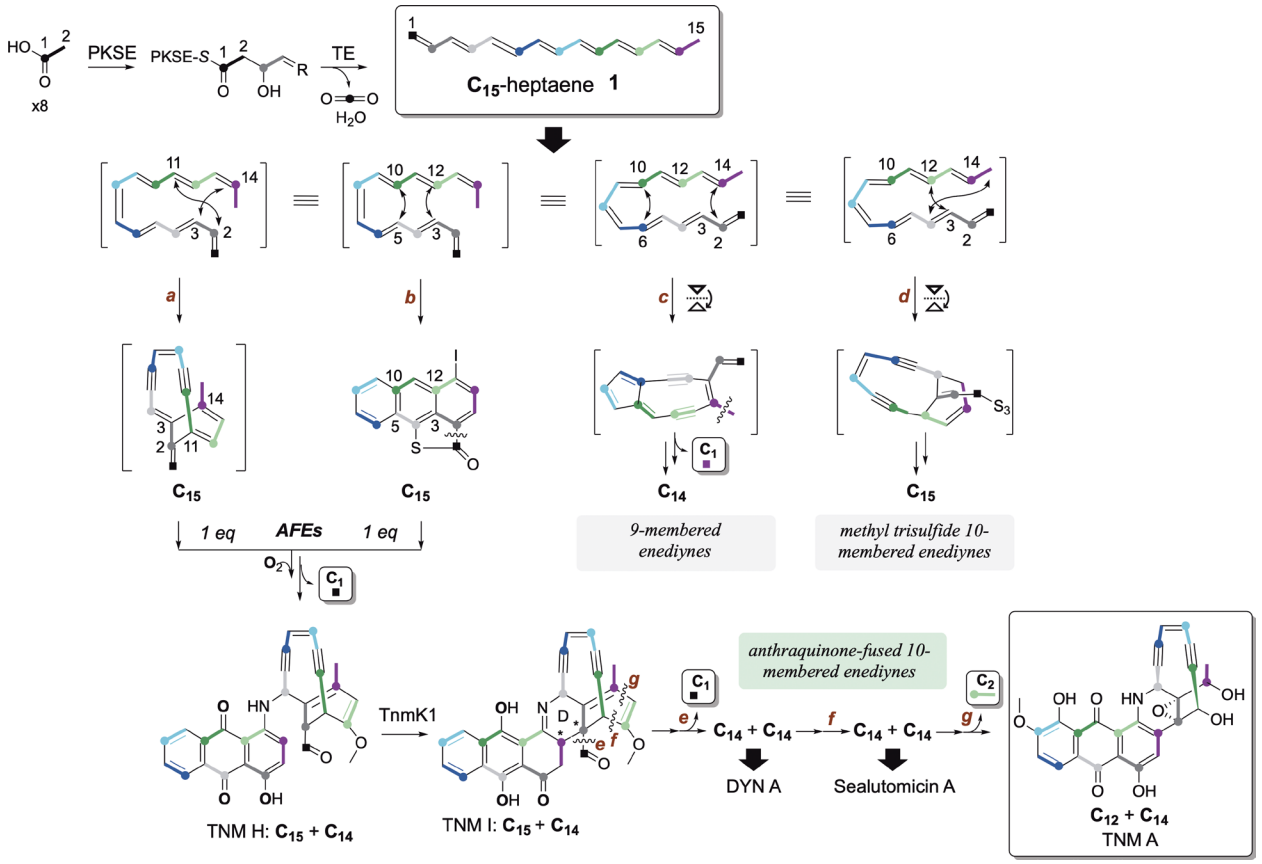

Fig. 5. Proposed biosynthesis of all enediynes starting from the common intermediate 1. The thick bond with a circle represents a C_2 unit originating from an intact acetate, and the black square designates an unpaired carbon originating from C2 of acetate. The C2 units are color coded to depict each acetate unit incorporated by PKSE and to demonstrate the regiochemical orientation in the final products. Structures shown in brackets are hypothetical and used to depict the folding pattern and cyclization of the enediyne cores. *stereochemistry defined in ref. 37.

cyclization and attachment remains unknown, the discovery of anthracene-containing metabolites bonded to the enediyne core via the ring junction N atom (34, 46) and the inability to incorporate a free anthraquinone into DYN A (31) suggests the enediyne core component is linked prior to quinone formation. The converged intermediate TNM H is then converted to TNM I by TnmK1 to establish the characteristic piperidine (D ring) of all AFEs. Subsequently, the aldehyde functionality (formerly C1 of **1**) is excised—accounting for the loss of one C atom originating from C2 of acetate—to give the C_{14} bridged bicycle found in the DYN A structure. Multiple TNM A analogues (e.g., TNM B–G; *SI Appendix*, Fig. S15) have been isolated from mutant strains that contain a C_{14}-containing monocyclic enediyne core reminiscent of sealutomicin A (36, 38, 39), suggesting that carbon–carbon bond breaking in the F ring (formerly C11-C12 of **1**) occurs next to give a C_{14} monocyclic core**.** A second C–C bond break (formerly C13-C14 of **1**)—accounting for two C atoms derived from one acetate unit—occurs to provide the C_{12} scaffold of several AFEs including TNM A. The finding here that **1** is a discrete intermediate will now facilitate studies toward elucidating the early biosynthetic steps, including how such a hydrophobic, completely deoxygenated intermediate is initially processed and cyclized to yield the bridged bicyclic enediyne core that is the proposed precursor of all AFEs.

In addition to the enediyne core precursor, the labeling studies have directly demonstrated that the PKSE/TE product **1** is also a discrete, noncyclized precursor of the anthraquinone moiety of TNM A. A C_{15} γ-thiolactone-fused iodoanthracene was previously identified as the first cyclized precursor of the anthraquinone of AFEs (31, 34), suggesting **1** is first converted to the γ-thiolactone-fused iodoanthracene prior to combining with the enediyne core (*SI Appendix*, Fig. S1 and Fig. 5). By comparing the labeling patterns of **1** and the anthracene intermediate, it can be inferred that processing of **1** will include C5–C10 and C3–C12 cyclizations (Fig. 5, path b). Interestingly, the latter cyclization regiospecificity—in addition to an unusual C-S bond formation at C1 of **1**—is realized during the biosynthesis of the enediyne core of calicheamicin γ_1 and esperamicin A_1, suggesting potential shared downstream biosynthetic steps between 10-membered enediyne classes. In contrast to the calicheamicin γ_1 and esperamicin A_1 enediyne cores, however, C1 is ultimately excised during anthraquinone biosynthesis. Oxidation (via oxygenases) of the anthraquinone precursor, which likely occurs after coupling to the enediyne core, ultimately yields TNM H, which we hypothesize is an anthraquinone-containing biosynthetic intermediate for all AFEs. Notably, this anthraquinone biosynthetic logic is different than the established paradigm in bacteria (35, 47, 48). The biosynthesis of bacterial anthraquinones has hitherto only been known to be initiated by a type II PKS, consisting of minimally three essential proteins: a ketosynthase α (KSα), KSβ (also known as chain length factor), and ACP, that generate a nonreduced, poly-β-ketoacyl-*S*-ACP product (*SI Appendix*, Fig. S16). An aromatase/cyclase and cyclase then catalyze aldol condensations of the thioesterified intermediate to yield the initial monocyclic and bicyclic structures, respectively, ultimately forming an anthrone that is oxidized to the anthraquinone (49, 50). Contrastingly, anthraquinones from AFEs are derived from the product of PKSE, which is a single, multidomain protein containing a KS, acyltransferase, ACP, ketoreductase, dehydratase, and phosphopantetheinyltransferase domains (*SI Appendix*, Fig. S16) (19). Iterative

decarboxylative condensation with concomitant ketoreduction and dehydration yields a mostly reduced, thioesterified octaketide, 3-hydroxy-4,6,8,10,12,14-hexadecahexenoyl-*S*-PKSE. The free-standing enediyne TE, which is proposed to be highly selective for C_{16} chain length of the PKSE-tethered product, then catalyzes the formation of **1**. In addition to different PKS architecture and required protein functions, **1**—unlike the poly-β-ketoacyl-*S*-ACP—lacks O atoms, suggesting that the cyclizations may proceed by a mechanism that is distinct from an aldol condensation. Finally, both O atoms of the quinone originate from O_2. This clearly contrasts the type II PKS paradigm where one of the two O atoms of the quinone is derived from acetate. These unique O-labeling patterns can now be exploited to facilitate forward and reverse genomics to find anthraquinones and establish the biosynthetic origin, respectively.

We previously reported that PKSE chemistry does not direct the biosynthetic divergence between the enediyne cores among the three subclasses of enediynes (20). Notably, all PKSE/TE pairs regardless of source or assay have been shown to generate **1**. We have taken advantage of this here using the PKSE (SgcE) and TE (SgcE10) pair from a 9-membered enediyne biosynthetic pathway to chemically cross complement and restore the production of the AFEs DYN A and TNM A to their respective PKSE mutant strains. Furthermore, we have shown that this transformation is dependent upon the inclusion of SgcE10, and TEs from the calicheamicin γ_1 and DYN A biosynthetic pathways can function with SgcE to achieve the same outcome as the canonical TE (i.e., SgcE10). These data, along with the structural analysis of TEs that is consistent with an identical function across the subclasses (27–29), further support that PKSE chemistry is agnostic with respect to pathway divergence and strongly suggests that the enediyne cores of the 9-membered enediynes and the methyl trisulfide-containing 10-membered enediynes also originate from the C_{15} polyene **1**. Interestingly, like the biosynthesis of the enediyne core of AFEs, this would require two C–C bond forming events for both. Based on the previously identified labeling pattern for neocarzinostatin, the biosynthesis of the enediyne core of the 9-membered fused bicyclic core starting from **1** would require the formation of C–C bonds between C2–C14 and C6–C10 (Fig. 5*A*, path c). Similarly to the initial processing of the enediyne core of the proposed universal AFE precursor TNM H, a terminal C (formerly C15 of **1**) is excised to establish the observed C_{14} structure of the 9-membered enediynes. Comparatively, the known labeling pattern for esperamicin A_1 suggests that an intact **1** is incorporated, which would require C–C bonds between C3–C12 and C4–C15 to form the distinct C_{15} bridged bicyclic core of this subclass (Fig. 5*A*, path d) without the need for any C–C bond breaking events. Studies are now ongoing to adopt the chemical complementation platform to the other enediyne subclasses to probe the proposed universal nature of **1** in enediyne biosynthesis.

In conclusion, a unifying pathway for enediyne core biosynthesis is put forth that features divergence from a shared polyketide **1**. Equally significant, an unprecedented logic for generating anthraquinone-type aromatic polyketides has been established that features **1** as the precursor, thereby suggesting several unusual post-PKSE/TE cyclization and oxidation events. Importantly, the proposed processing of **1** into the different enediyne cores and anthraquinone moiety (Fig. 5) is entirely consistent with our data, prior feeding experiments, and past genomic and biochemical studies. The ability to feed small molecule precursors such as **1**, realized here by developing and implementing a synthetic biology-chemical complementation platform, now provides the foundation for exploring the intriguing shared and/or unique catalytic transformations invoked downstream. For the enediyne core, this includes the chemically intriguing oxidative event(s) generating the reactive triple bonds, which remains a mystery.

Methods

General. Isotopically labeled reagents and OminPur® Pronase E (4,000 U/mg) were purchased from Sigma Aldrich. GCMS data were acquired with an Agilent 7890 GC with a 30-m × 250-μm × 0.25-mm HP 5-ms UI capillary column and Agilent G7081B MSD. High-resolution mass spectrometry data were acquired with an Agilent 6230 TOF LC/MS System (Agilent Technologies) equipped with a ZORBAX Eclipse XDB C18 column (5 μm, 150 × 4.6 mm). NMR data were recorded at 400 MHz for ^{1}H and 100 MHz for ^{13}C with a Varian Inova NMR spectrometer (Agilent). ^{13}C NMR for [2,4,6,8,10,12,14,17,19,21,23,25,27-^{13}C]TNM A was acquired using a Bruker NEO 600 MHz (14.1 T) NMR spectrometer equipped with four-channel, 24 slot SampleCase, and a triple resonance (HCN) CryoProbe. The gene encoding SgcE was coexpressed in pET30Xa-LIC vector with SgcE10 in pCDF-F2-EK-LIC vector as previously described (19). The gene encoding DynE8 was coexpressed in pET30Xa-LIC vector with SgcE10 in pCDF-2-EK-LIC vector. The TNM A-producing strain *Streptomyces sp.* CB03234 and the generation of the PKSE (Δ*tmnE*) mutant strain SB20001 were previously described (16). The DYN A-producing strain *Micromonospora chersina* ATCC 53710 and the generation of the PKSE (Δ*dynE7*) mutant strain were previously described (15).

Production of TNM A. *Streptomyces* sp. CB03234 was grown in three 250-mL conical flasks containing 50 mL Tryptic soy broth liquid media at 28 °C and 250 rpm for 48 h. The seed culture (5 mL) was transferred to 250-mL conical flasks containing 50 mL production media consisting of soluble starch 10 g/L, Pharmamedia 5 g/L, $CaCO_3$ 1 g/L, $CuSO_4 \bullet 5H_2O$ 0.05 g/L, and KI 0.5 mg/L, adjusted to pH 7.2. After 72 h in production media, DAX-8 resin (1% w/v) was added. The resulting culture was incubated at 28 °C and 250 rpm for 6 d prior to harvesting. The DAX-8 resin was extracted twice with ethyl acetate. The combined ethyl acetate extract was concentrated in vacuum, and TNM A was partially purified by flash chromatography with silica gel eluting with 5% MeOH in $CHCl_3$. Fractions containing TNM A were combined, dried, dissolved in MeOH, and further fractionated by Sephadex LH-20. The TNM A-containing fractions were combined and loaded on a semipreparative HPLC using an Apollo C18 column (5 μm, 250 mm × 10 mm) with a flow rate of 3.2 mL/min using a 50-min gradient from 30% acetonitrile in water to 70% acetonitrile in water to give pure TNM A**.**

Production of DYN A. *Micromonospora chersina* was grown in two 250-mL conical flasks containing 50 mL seed media consisting of soluble starch 10 g/L, Pharmamedia 5 g/L, $CaCO_3$ 1 g/L, $CuSO_4 \bullet 5H_2O$ 0.05 g/L, KI 0.5 mg/L, adjusted to pH 7.2 at 28 °C and 250 rpm for 7 d. The seed culture (2 mL) was transferred to 250-mL conical flasks containing 50 mL production media consisting of soluble starch 10 g/L, Pharmamedia 5 g/L, $CaCO_3$ 1 g/L, $CuSO_4 \bullet 5H_2O$ 0.05 g/L, KI 0.5 mg/L, adjusted to pH 7.2. After 72 h in production media, DAX-8 resin (1% w/v) was added. The resulting culture was incubated at 28 °C and 250 rpm for 6 d prior to harvesting. The DAX-8 resin was extracted twice with ethyl acetate. The combined ethyl acetate extract was concentrated in vacuum, and DYN A was partially purified by flash chromatography with silica gel eluting with 5% MeOH in $CHCl_3$. Fractions containing DYN A were combined, dried, dissolved in DMSO, and further fractionated by Sephadex LH-20. The DYN A-containing fractions were subsequently combined and loaded on a semipreparative HPLC using an Apollo C18 column (5 μm, 250 mm × 10 mm) with a flow rate of 2 mL/min using a 30-min isocratic elution of 65% acetonitrile in water to give pure DYN A**.**

Coexpression of *sgcE* and *sgcE10* for One Production in *E. coli*. The plasmid pET30Xa-LIC/*sgcE* and pCDF-F2-EK-LIC/*sgcE10* were cotransformed into *E. coli* BL21(DE3) cells, which were plated on LB agar supplemented with 50 μg/mL kanamycin and 50 μg/mL streptomycin. After overnight incubation at 37 °C, a single colony was used to inoculate 5 mL LB medium supplemented with 50 μg/mL kanamycin and 50 μg/mL streptomycin. The culture was incubated overnight at 37 °C and 250 rpm prior to complete transfer to 500 mL fresh LB supplemented with 50 μg/mL kanamycin and 50 μg/mL streptomycin. The culture was incubated at 18 °C and 250 rpm until the optical density at 600 nm reached 0.5 to 0.6 (~6 h), at which time coexpression was induced with the addition of IPTG (final

concentration 0.1 mM). After incubation in the dark at 18 °C and 250 rpm for 36 additional hours, the cells were centrifuged 30 min at 8,000 rpm and 4 °C for 30 min. After decanting, the cell pellet was transferred into a new 50-mL centrifuge tube and stored at −20 °C until further use.

For ^{13}C enrichment *E. coli* was cultured as above except ^{13}C-labeled sodium acetate was added to a final concentration of 1.0 mg/mL at the time of IPTG induction. After 12 h, an additional aliquot of ^{13}C-labeled sodium acetate (final concentration 2 mg/mL) was added. The culture was grown for 12 h before collecting the cell pellet.

Chemical Complementation of SB20001. Strain SB20001 was grown in 250-mL flask containing 50 mL TSB liquid medium. After 48 h at 28°C and 250 rpm, 5 mL seed culture was inoculated into a 250-mL flask containing 50 mL production medium. Frozen *E. coli* pellet (2 g) coexpressing *sgcE* and *sgcE10* was resuspended and thoroughly washed once with 30 mL water and twice with 30 mL 50 mM phosphate buffer (pH 7.2). The washed pellet was resuspended in 30 mL 50 mM phosphate buffer (pH 7.2) and sonicated for 2 min with 10-s pulse on and 50-s pulse off (with 40% amplitude) on ice. Ten mL (2400AU) of the sonicated, resuspended pellet was added to the SB20001 culture after 24-h incubation in the production medium. DAX-8 resin (1% w/v) was added after 72 h from the start of the production culture. The resulting culture was incubated at 28 °C and 250 rpm for four more days prior to harvesting by centrifugation. Ethyl acetate (50 mL) was added to 50 mL supernatant, and the organic extract was recovered, concentrated under vacuum, and dissolved in MeOH for HPLC analysis.

For GCMS analysis of the polyene products, the washed *E. coli* pellet was resuspended in 10 mL 50 mM phosphate buffer (pH 7.2) and extracted with an equal volume of ethyl acetate for 2 h at room temperature and 50 rpm in the dark. The ethyl acetate layer was collected and mostly removed using a nitrogen evaporator, redissolved in 100 μL chloroform, and syringe filtered. The samples were analyzed by GCMS using injections of 5 mL in a splitless mode. Column temperature was initially 70 °C and held for 2 min, increasing to 240 °C at 4 °C/min for 59.5 min. An electron impact ionization system was used with mass range set to 50 to 500 *m/z* and a filament delay of 4 min. Helium was the carrier gas at a flow rate of 1 mL/min. The temperatures of the injector, the interface, and the liner were maintained at 250 °C.

For LCMS analysis, the column was equilibrated with solvent A (H_2O with 0.1% HCO_2H) and B (CH_3CN) (95:5, v/v), and samples were eluted with a linear gradient (0 to 16 min, 5 to 100% B; 16 to 20 min, 100% B; 20 to 30 min, 100 to 5% B) at a flow rate of 0.3 mL per min with both diode array and mass detectors.

Ethyl Acetate Extraction of *E. coli* Coexpressing *sgcE* and *sgcE10* for Feeding. *E. coli* pellet (5.5 g) expressing *sgcE* and *sgcE10* was extracted with ethyl acetate overnight in the dark. The ethyl acetate layer was separated and 500 μL DMSO was added. The ethyl acetate layer was removed under vacuum, and 100 μL DMSO extract of polyene was used for feeding SB20001 at 96 h.

Protease Treatment of Sonicated Lysate of *E. coli* Coexpressing *sgcE* and *sgcE10*. A 500 mL culture of *E. coli* coexpressing sgcE and *sgcE10* was centrifuged at 8,000 rpm for 20 min at 4 °C in the dark to give 2.44 g wet pellet. The wet pellet was washed once with water (30 mL) and twice with 30 mL 50 mM phosphate buffer (pH 7.2). The pellet was resuspended in 30 mL 50 mM phosphate buffer (pH 7.2) and sonicated for 2 min with 10-s pulse on and 50-s pulse off (with 40% amplitude) on ice. A portion (10 mL) of the sonicated sample was kept at room temperature (or 4 °C) for 24 h and directly fed to a 50 mL culture of SB2001. The remaining 20 mL was treated with pronase E solution (final concentration of 1.9 U/μL) for 24 h at room temperature in the dark. Two 50 mL cultures of SB2001were independently fed with 10 mL protease-treated sample. The remaining sample was retained for SDS–PAGE analysis.

Analysis for Isotopic Enrichment. Processing of the GCMS data for **1** and the LCMS data for TNM A is provided in *SI Appendix* available online.

Data, Materials, and Software Availability. All study data are included in the article and/or *SI Appendix*.

ACKNOWLEDGMENTS. This work was supported by the National Cancer Institute grants CA217255 (J.S.T., G.N.P., and S.G.V.L.) and CA204484 (B.S.), the National Institute of General Medicine grant GM134954 (B.S.), the National Institute of General Medicine fellowship GM134688 (E.K.), the NIH Center of Biomedical Research Excellence (COBRE) in Pharmaceutical Research and Innovation grant P20GM130456 (J.S.T.), and the National Center for Advancing Translational Sciences grants UL1TR000117 and UL1TR001998 (J.S.T.), and the University of Kentucky College of Pharmacy. Some NMR data were acquired on a Bruker AVANCE NEO 600 MHz high-performance digital NMR spectrometer funded by NIH grant S10OD28690. We thank Vivekanandan Subramanian and the College of Pharmacy PharmNMR Center for analytical support.

Author affiliations: [a]Department of Pharmaceutical Sciences, College of Pharmacy, University of Kentucky, Lexington, KY 40536; [b]Department of Physiology, College of Medicine, University of Kentucky, Lexington, KY 40536; [c]Department of Microbiology, Immunology and Molecular Genetics, College of Medicine, University of Kentucky, Lexington, KY 40536; [d]Department of Chemistry, The Herbert Wertheim UF Scripps Institute for Biomedical Innovation & Technology, University of Florida, Jupiter, FL 33458; [e]Natural Products Discovery Center, The Herbert Wertheim UF Scripps Institute for Biomedical Innovation & Technology, University of Florida, Jupiter, FL 33458; [f]Department of BioSciences, Rice University, Houston, TX 77005; [g]Department of Molecular Medicine, The Herbert Wertheim UF Scripps Institute for Biomedical Innovation & Technology, University of Florida, Jupiter, FL 33458; and [h]Skaggs Graduate School of Chemical and Biological Sciences, Scripps Research, Jupiter, FL 33458

1. S. G. Van Lanen, B. Shen, Biosynthesis of enediyne antitumor antibiotics. *Curr. Top. Med. Chem.* **8**, 448–459 (2008).
2. A. Adhikari, C. N. Teijaro, C. A. Townsend, B. Shen, "Biosynthesis of enediyne natural products" in *Comprehensive Natural Products III: Chemistry and Biology*, H.-W. Liu, T. P. Begley, Eds. (Elsevier, 2020), pp. 365–414.
3. U. Galm *et al.*, Antitumor antibiotics: Bleomycin, enediynes, and mitomycin. *Chem. Rev.* **105**, 739–758 (2005).
4. J. D. Rudolf, X. Yan, B. Shen, Genome neighborhood network reveals insights into enediyne biosynthesis and facilitates prediction and prioritization for discovery. *J. Ind. Microbiol. Biotechnol.* **43**, 261–276 (2016).
5. H. Maeda, SMANCS and polymer-conjugated macromolecular drugs: Advantages in cancer chemotherapy. *Adv. Drug Deliver. Rev.* **46**, 169–185 (2001).
6. A. Adhikari, B. Shen, C. Rader, Challenges and opportunities to develop enediyne natural products as payloads for antibody-drug conjugates. *Antib. Ther.* **4**, 1–15 (2021).
7. Y. Tokiwa *et al.*, Biosynthesis of dynemicin A, a 3-ene-1,5-diyne antitumor antibiotic. *J. Am. Chem. Soc.* **114**, 4107–4110 (1992).
8. G. L. Ma *et al.*, Pathway retrofitting yields insights into the biosynthesis of anthraquinone-fused enediynes. *J. Am. Chem. Soc.* **143**, 11500–11509 (2021).
9. O. D. Hensens, J.-L. Giner, I. H. Goldberg, I. H., Biosynthesis of NCS Chrom A, the chromophore of the antitumor antibiotic neocarzinostatin. *J. Am. Chem. Soc.* **111**, 3295–3299 (1989).
10. K. S. Lam *et al.*, Biosynthesis of esperamicin A1, an enediyne antitumor antibiotic. *J. Am. Chem. Soc.* **115**, 12340–12345 (1993).
11. W. Liu, S. D. Christenson, S. Standage, B. Shen, Biosynthesis of the enediyne antitumor antibiotic C-1027. *Science* **297**, 1170–1173 (2002).
12. J. Ahlert *et al.*, The calicheamicin gene cluster and its iterative type I enediyne PKS. *Science* **297**, 1173–1176 (2002).
13. W. Liu *et al.*, The neocarzinostatin biosynthetic gene cluster from *Streptomyces carzinostaticus* ATCC 15944 involving two iterative type I polyketide synthases. *Chem. Biol.* **12**, 293–302 (2005).
14. S. G. Van Lanen, T.-J. Oh, W. Liu, E. Wendt-Pienkowski, B. Shen, Characterization of the maduropeptin biosynthetic gene cluster from *Actinomadura madurae* ATCC 39144 supporting a unifying paradigm for enediyne biosynthesis. *J. Am. Chem. Soc.* **129**, 13082–13094 (2007).
15. Q. Gao, J. S. Thorson, The biosynthetic genes encoding for the production of the dynemicin enediyne core in *Micromonospora chersina* ATCC 53710. *FEMS Microbiol.* **282**, 105–114 (2008).
16. X. Yan *et al.*, Strain prioritization and genome mining for enediyne natural products. *mBio* **7**, e02104–16 (2016).
17. W. Liu *et al.*, Rapid PCR amplification of minimal enediyne polyketide synthase cassettes leads to a predictive familial classification model. *Proc. Natl. Acad. Sci. U.S.A.* **100**, 11959–11961 (2003).
18. Zazopoulos *et al.*, A genomics-guided approach for discovering and expressing cryptic metabolic pathways. *Nat. Biotech.* **21**, 1870190 (2003).
19. J. Zhang *et al.*, A phosphopantetheinylating polyketide synthase producing a linear polyene to initiate enediyne antitumor antibiotic biosynthesis. *Proc. Natl. Acad. Sci. U.S.A.* **105**, 1460–1465 (2008).
20. G. P. Horsman, Y. Chen, J. S. Thorson, B. Shen, Polyketide synthase chemistry does not direct biosynthetic divergence between 9- and 10-membered enediynes. *Proc. Natl. Acad. Sci. U.S.A.* **107**, 11331–11335 (2010).
21. R. Kong *et al.*, Characterization of a carbonyl-conjugated polyene precursor in 10-membered enediyne biosynthesis. *J. Am. Chem. Soc.* **130**, 8142–8143 (2008).
22. H. Sun *et al.*, Products of the iterative polyketide synthases in 9- and 10-membered enediyne biosynthesis. *Chem. Commun.* **21**, 7399–7401 (2009).
23. X. Chen, Z.-F. Guo, P. Man Lai, K. Hung Sze, Z. Guo, Identification of a nonaketide product for the iterative polyketide synthase in biosynthesis of the nine-membered enediyne C-1027. *Angew. Chem. Int. Ed.* **49**, 7926–7928 (2010).
24. K. Belecki, J. M. Crawford, C. A. Townsend, Production of octaketide polyenes by the calicheamicin polyketide synthase Cal E8: Implications for the biosynthesis of enediyne core structures. *J. Am. Chem. Soc.* **131**, 12564–12566 (2009).

25. K. Belecki, C. A. Townsend, Environmental control of the calicheamicin polyketide synthase leads to detection of a programmed octaketide and a proposal for enediyne biosynthesis. *Angew. Chem. Int. Ed.* **51**, 11316–11319 (2012).
26. K. Belecki, C. A. Townsend, Biochemical determination of enzyme-bound metabolites: Preferential accumulation of a programmed octaketide on the enediyne polyketide synthase CalE8. *J. Am. Chem. Soc.* **135**, 14339–14348 (2013).
27. C. W. Liew *et al.*, Induced-fit upon ligand binding revealed by crystal structures of the hot-dog fold thioesterase in dynemicin biosynthesis. *J. Mol. Biol.* **404**, 291–306 (2010).
28. M. Kotaka *et al.*, Structure and catalytic mechanism of the thioesterase CalE7 in enediyne biosynthesis. *J. Biol. Chem.* **284**, 15739–15739 (2009).
29. T. Annaval *et al.*, Crystal structure of thioesterase SgcE10 supporting common polyene intermediates in 9- and 10-membered enediyne core biosynthesis. *ACS Omega* **2**, 5159–5169 (2017).
30. R. Cohen, C. A. Townsend, A dual role for a polyketide synthase in dynemicin enediyne and anthraquinone biosynthesis. *Nat. Chem.* **10**, 231–236 (2018).
31. D. R. Cohen, C. A. Townsend, Characterization of an anthracene intermediate in dynemicin biosynthesis. *Angew. Chem. Int. Ed.* **57**, 5650–5654 (2018).
32. X. Yan, Anthraquinone-fused enediynes: Discovery, biosynthesis and development. *Nat. Prod. Rep.* **39**, 703–728 (2022).
33. J. Pan *et al.*, Discovery of pentaene polyols by activation of an enediyne gene cluster: Biosynthetic implications for 9-membered enediyne core structures. *Chem. Sci.* **13**, 13475–13481 (2022), 10.1039/D2SC04379C.
34. Z. J. Low *et al.*, Sungeidines from a non-canonical enediyne biosynthetic pathway. *J. Am. Chem. Soc.* **142**, 1673–1679 (2020).
35. B. Shen, Biosynthesis of aromatic polyketides. *Curr. Top. Chem.* **209**, 1–51 (2000).
36. X. Yan *et al.*, Comparative studies of the biosynthetic gene clusters for anthraquinone-fused enediynes shedding light into the tailoring steps of tiancimyicin biosynthesis. *Org. Lett.* **20**, 5918–5921 (2018).
37. C. Gui *et al.*, Intramolecular C-C bond formation links anthraquinone and enediyne scaffolds in tiancimycin biosynthesis. *J. Am. Chem. Soc.* **144**, 20452–20462 (2022).
38. T. Annaval *et al.*, Cytochrome P450 hydroxylase TnmL catalyzing sequential hydroxylation with an additional proofreading activity in tiancimycin biosynthesis. *ACS Chem. Biol.* **16**, 1172–1178 (2021).
39. X. Yan *et al.*, Comparative studies of the biosynthetic gene clusters for anthraquinone-fused enediynes shedding light into the tailoring steps of tiancimycin biosynthesis. *Org. Lett.* **20**, 5918–5921 (2018).
40. P. Nayler, M. C. Whiting, Researches on polyenes. Part III. The synthesis and light absorption of dimethylpolyenes. *J. Chem. Soc.* **1955**, 3037–3047 (1955).
41. K. Knoll, R. R. Schrock, Preparation of tert-butyl-capped polyenes containing up to 15 double bonds. *J. Am. Chem. Soc.* **111**, 7989–8004 (1989).
42. K. L. D'Amico, C. Manos, R. L. Christensen, Electronic energy levels in a homologous series of unsubstitued linear polyenes. *J. Am. Chem. Soc.* **102**, 1777–1782 (1980).
43. D. Schwarzer, H. D. Mootz, U. Linne, M. A. Marahiel, Regeneration of misprimed nonribosomal peptide synthetases by type II thioesterases. *Prod. Natl. Acad. Sci. U.S.A.* **99**, 14083–14088 (2002).
44. B. S. Kim, T. A. Cropp, B. J. Beck, D. H. Sherman, K. A. Reynolds, Biochemical evidence for an editing role of thioesterase II in the biosynthesis of the polyketide pikromycin. *J. Biol. Chem.* **277**, 48028–48034 (2002).
45. F. Pourmasoumi *et al.*, Proof-reading thioesterase boosts activity of engineered nonribosomal peptide synthetase. *ACS Chem. Biol.* **17**, 2382–2388 (2022).
46. D. R. Cohen, C. A. Townsend, C—N-Coupled metabolites yield insights into dynemicin A biosynthesis. *ChemBioChem* **21**, 2137–2142 (2020).
47. W. Zhang, Y. Li, Y. Tang, Engineered biosynthesis of bacterial aromatic polyketides in *Escherichia coli*. *Proc. Natl. Acad. Sci. U.S.A.* **105**, 20683–20688 (2008).
48. M. Cummings *et al.*, Assembling a plug-and-play production line for combinatorial biosynthesis of aromatic polyketides in *Escherichia coli*. *PLoS Biol.* **17**, e3000347 (2019).
49. R. Thomas, A biosynthetic classification of fungal and streptomycete fused-ring aromatic polyketides. *ChemBioChem* **2**, 612–627 (2001).
50. G. Caldara-Festin *et al.*, Structural and functional analysis of two di-domain aromatase/cyclases from type II polyketide synthases. *Proc. Natl. Acad. Sci. U.S.A.* **112**, E6844–E6851 (2015).